Predictability of the Moisture Regime Associated with the Preonset of Sahelian Rainfall

Roberto J. Mera and Fredrick H.M. Semazzi
North Carolina State University
Corresponding author: rjmera@ncsu.edu

Introduction

Meningitis and Climate Information

The risk of mortality from climate-related diseases and their impact on socio-economic stability and sustainable development is one of the most important areas of study across sub-Saharan Africa. Meningococcal meningitis, for example, has been noted in Africa for the past 100 years, where Neisseria meningitides is endemic and periodically epidemic (Greenwood 1999). Each year, meningitis epidemics affect about 250,000 people, causing an average of 25,000 fatalities. The World Health Organization (WHO) and the Meningitis Environmental Risks Information Technologies (MERIT) initiative have determined that the Meningitis Belt (a geographic area of Sub-Saharan Africa prone to disease epidemics that ranges from the western coast of Africa east to Ethiopia) is vulnerable to a number of risk factors that include climate, socio-demographic and immunologic. The disease cases start increasing during the beginning of the dry season (January) and experience a sharp decrease with the advent of the monsoon.

Meningitis epidemics tend to occur in sectors of West Africa that exhibit particular environmental characteristics. The most robust and actionable climate/meningitis relationship arises from the strong correlation between the start of the rainy season and the abrupt decline in the transmission of the disease (Molesworth et al., 2003). Ongoing research also indicates that along with moisture (relative and absolute humidity), incidence of the disease can also be affected by land-cover type (e.g. arid, semi-arid, tropical forest), dust loading in the atmosphere, surface temperature, and enhanced northerly (Harmattan) winds.

Climate information for the MERIT program has three different temporal scales of relevance: interannual, seasonal, and intraseasonal. The interannual timescale is important for decisions regarding vaccine production a full year in advance of the next meningitis season. Seasonal climate information may be applied for logistical consideration (distribution of vaccine stockpiles, transportation, personnel) ahead of changes in the environment that can influence epidemic patterns. Intraseasonal or short-term weather forecasts are designed to minimize meningitis incidence by providing 1-14 day weather forecasts to target dissemination of scarce vaccine. The aim of short-term forecasts is to diagnose environmental conditions a week in advance that could push a district in “alert” into a full epidemic. The knowledge may be used to shift resources from a high-humidity district (in which the disease spread is lessening) to a dry area still prone to disease spread.

An important recent development in MERIT that is of special significance for the proposed study has been the construction of a refined decision tree with specific operational criteria to lower the "action threshold" for vaccine implementation. The objective is to define criteria consisting of several possible outcomes that determine vaccination actions. This decision tree, however, does not include climate information. Subsequent discussions were aimed at integrating the environmental factors into the decision tree. Our aim is to address the climate factors pertinent to meningitis mitigation at the appropriate timescales. The focus of our research is therefore to identify the predictability of atmospheric moisture ahead of the monsoon, its sources and variability. Our study will serve as a compliment to work currently under development at the University Corporation for Atmospheric Research (UCAR) by evaluating the skill of the Weather Research and Forecasting Model (WRF) and other model forecasts of weather variables at spatial resolutions (district level) and timescales that are relevant to meningitis management in the region.

Pre-onset of Sahelian Rains

The preonset period of the West African Monsoon (WAM) is defined as the arrival of the intertropical front (ITF) at 15 N, where the confluence line between moist southwesterly monsoon winds and dry northeasterly Harmattan occurs (Sultan and Janicot 2000; Le Barbe et al. 2002, Sultan and Janicot, 2003). This brings sufficient moisture for isolated convective systems to develop in the Sudano–Sahelian zone ahead of the Intertropical Convergence Zone (ITCZ), which during late May / early June is located at 5N. Dynamics associated with the Saharan Heat Low (SHL) dominates the continental region during this time period. Also during this time, isolated convective systems appear over the continent, resulting in an apparent expansion of the ITCZ.

The dynamics of the monsoon winds are controlled by the pressure gradient between the heat low located over the ITF and oceanic high pressures (e.g. Santa Helena anticyclone), while the Harmattan is modulated by pressure gradients created by the SHL and the Azores and Lybian anticyclones (Sultan and Janicot, 2003). Moisture advection into West Africa throughout the dry season and the pre-onset of the monsoon can have a significant impact on the timing of the monsoon “jump” as described by Hagos and Cook (2007). It was suggested by Sultan and Janicot (2000) and Le Barbe et al. (2002) that the “jump” can be characterized as an acceleration of the seasonal cycle triggered by westward propagating convective events.

The variability of the pre-onset stage of monsoon development is one of the factors that affect the moisture regime of the region in the days and weeks prior to the onset of the WAM. Our study aims to understand the moisture conditions that precede the WAM on interannual, seasonal and intraseasonal time scales. More specifically, we focus on conditions at the surface where there is a robust, actionable relationship between meningitis mitigation and environmental conditions. Some of the more prevalent features that dictate the moisture content of the atmosphere during this time period include the evolution of sea surface temperatures (SSTs) in the Gulf of Guinea (VIzy and Cook, 2001; Okumura and Xie, 2004), the intensity of rainfall along the Gulf of Guinea as described in Lebel et al (2003), the diurnal cycle of the monsoon (Parker et al., 2005), mid-latitude disturbance incursions into the region (Knipppertz and Fink, 2009), transient convective systems (Flamant et al., 2007, 2009), modulation of the SHL and African Easterly Jet (AEJ) (Sultan and Janicot, 2003), the migration of the ITF (Lele and Lamb, 2009), and variance of orographically induced circulations (Drobinski et al., 2005).

We use parcel back-trajectory analysis using the National Centers for Environmental Prediction (NCEP) / National Center for Atmospheric Research (NCAR) reanalysis, as well as the Weather Research and Forecasting (WRF) model Version 3 as tools to diagnose the primary attributes that dictate predictability of the moisture regime as dictated above. Presented in this study are parcel trajectory analysis showing source regions for air masses over the Sahel, WRF model configuration (physics parameters, domains used), ensembling techniques utilized, simulation results highlighting the ability of WRF to capture diurnal and intraseasonal variability (transient convective events) of moisture, as well as comparison between WRF output, reanalysis data and in-situ observations and their relationship with meningitis attack rate.

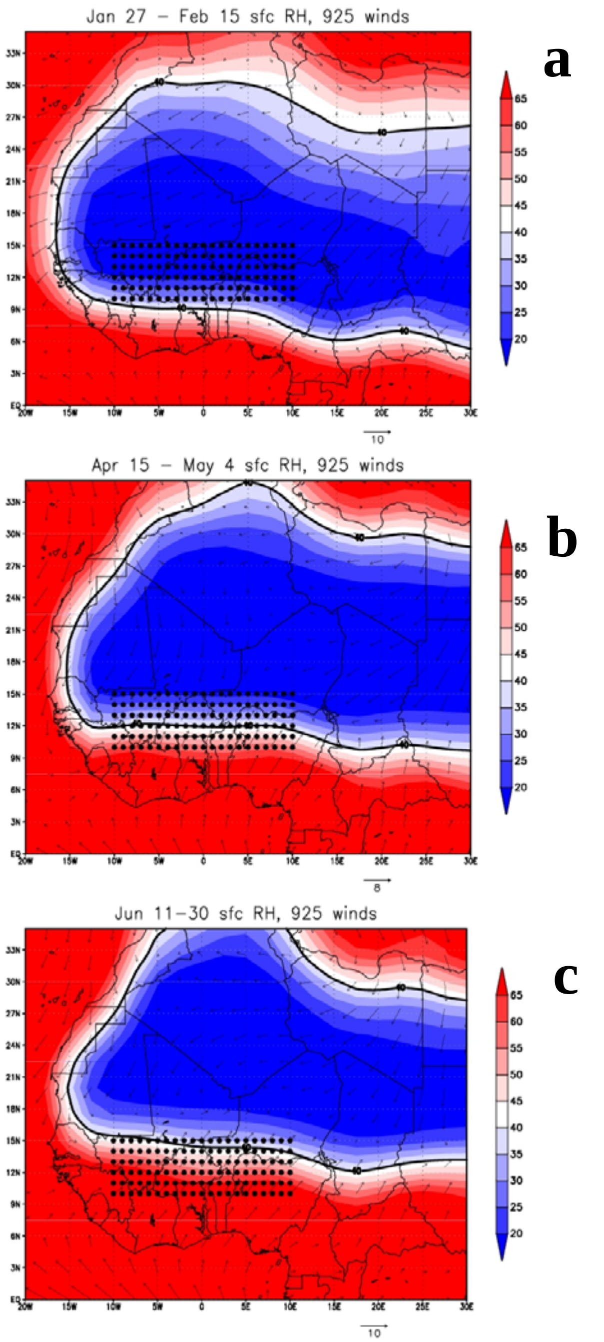

Figure 1. end point matrix, RH (%) during (a) Jan 27 – Feb 15, (b) Apr 16 – May 4, (c) Jun 11 -30. (2000-2008 averages)

Parcel Trajectory Analysis

In order to understand the overall mechanism for atmospheric moisture and air flow of the WAM during the boreal spring, we must first analyze the sources of air mass. Using a five day back-trajectory technique, and utilizing u and v wind components, as well as relative humidity (%) from the NCEP/NCAR reanalysis, we computed the sources of air parcels for the points bounded by 10W-10E and 10N-15N for the years 2000-2008. We have chosen 925 hPa level as our endpoint surface to circumvent noise generated in the reanalysis below 925 hPa, where parcels can intercept the ground (1000 hPa).

The length of the period used in this study reflects the need to analyze the dynamics at a daily scale due to the high variability of the system and because monthly averages tend to generalize conditions in the atmosphere to a degree that is unusable for the various applications (health, agriculture, etc.). For the sake of brevity, we have constricted our analysis to 19-day periods averaged before (P1, January 27 – February 15), during (P2, April 15 – May 4), and after (P3, June 11 – 30) the passage of the ITF through the region. This has allowed us to get an overall perspective of the climatology of the region during its different phases.

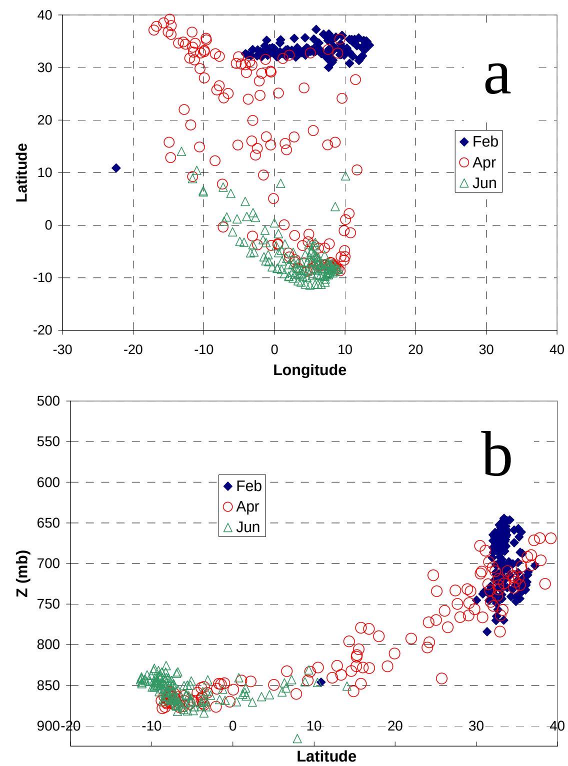

Figure 2. end point matrix, RH (%) during (a) Jan 27 – Feb 15, (b) Apr 16 – May 4, (c) Jun 11 -30. (2000-2008 averages)

As seen in figure 1, our region of study is completely immersed in the dry Saharan air during the early period (1a), partially within the moist environment of the WAM during P2 (1b), and almost entirely outside of the dry Saharan air in P3 (1c). Also note the strength and direction of the prevailing winds during these periods: strong northeasterlies for P1, a mix of northerly and northeasterlies for points north of the 40% line and WAM southwesterlies to the south for P2, and southwesterlies for P3 even for points that remain below 40%. We have chosen relative humidity (RH, %) as a variable to analyze because of its strong relationship with meningitis outbreaks. An important figure in the literature is the 40% threshold at which the dry, dusty Harmattan air is replaced by the moister Monsoon air mass (Besancenot et al., 1997). We will use this number as our indicator for the subsequent sections.

The source points vary in spatial scale both in their horizontal and vertical components. In figure 2a we show the horizontal distribution of source points for February (P1, solid diamonds), April (P2, circles), and June (P3, triangles). Figure 2b represents the vertical profile of the source points. Note that for P1, the majority of source points are tightly clustered north of 30N in North Africa. For P2, the spread of source points is much more scattered in nature and extends from north of 30N to the Atlantic Ocean south of the equator. In contrast with P1, the P3 source points are tightly clustered south of the equator over the Gulf of Guinea and points south. Vertically, source points during P1 are located in the mid to upper levels of the atmosphere (750-600 hPa), on average, with a wide spectrum of vertical source points during P2 (900 to 650 hPa), and strictly lower-level points during P3 (<800 hPa).

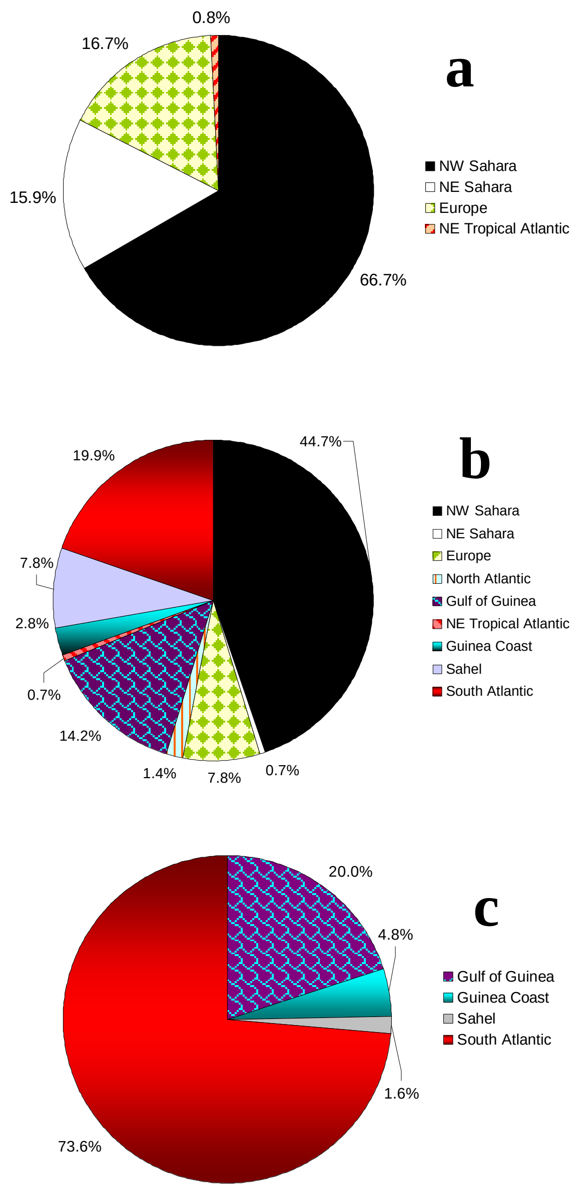

Figure 3. Distribution of air mass source regions, (a) P1, (b) P2 and (c) P3.

Further analysis of the source points for each of the periods shows the proportion of air parcels from each of the geographical areas (fig. 3) adjacent to and including the study region delineated in figure 1.During P1 (fig. 3a), the majority of parcels emanate from NW Sahara (66.7%), Europe (16.7%) and NE Sahara (15.9%). During P2 (fig. 3b), the majority of source points (44%) still have a source region in NW Sahara. The second highest density (20%) occurs over the South Atlantic region, with 14% for the Gulf of Guinea (GOG) and 8% within our box (Sahel). Smaller percentages represent areas like the GOG coast, North-east Tropical Atlantic (NETA) and NE Sahara. In contrast with P2, P3 (fig 3c) has the majority of source points (73%) located over the South Atlantic, and a smaller percentage (20%) from the GOG.

Model Configuration

We use the Weather Research and Forecasting Model (WRF) Version 3.0 as a predictive and analytical tool to gauge its ability to reproduce the environment over West Africa during the boreal spring. We selected the domains for our suite of experiments as displayed in figure 4. We use Mercator projection, a 90 km resolution for the outer domain and 30 km for the inner domain. The placement of the domain(s) conforms to the optimum configuration for important variables such as moisture advection, temperature, ITCZ location, orography. We use 5 point relaxation zone, a non-hydrostatic option and positive definite advection of moisture. The model uses NCEP Final Analyses (FNL) as boundary conditions and daily-updating sea surface temperatures (SSTs).

We conducted an ensemble of simulations for the March through June period in 2006 using a variety of physics parameters in order to discern the optimal configuration of packages for our purposes. We chose 2006 because of the significant amount of station observations during the African Monsoon Disciplinary Analysis (AMMA) (Redelsperger et al., 2006) and we use the station in Niamey, Niger (13°27'N, 02°06'E) to analyze model results at a specific location. The particular physics parameters tested include cumulus parameterization, surface layer option and surface physics, boundary layer option, soil layers, microphysics schemes and radiation schemes.

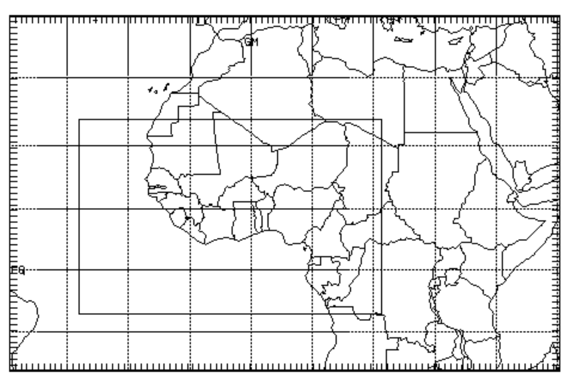

Figure 4. Inner and outer domain for WRF simulations

Ensemble Prediction

In this section we discuss the ensembling techniques utilized for seasonal analysis and real-time short and medium range forecast simulations. For the seasonal analysis we limit ensemble diversity to 8 combinations of physics schemes. This type of ensembling has yielded important variance in the simulation of RH that can be used for further refinement of physics parameterization. As we may discern from figure 5, there is a clear distinction between ensemble members using Thermal Diffusion for surface physics (WRF E8, E10 and E14) and Noah Land Surface Model (hereafter NLSM) option (WRF E1-5). We note that throughout the period May 1-29 the WRF simulations nearly continuously supersede the daily RH observations gathered at the Niamey station as can be shown when the average of the NLSM ensembles (dotted) is compared to the observed (solid).

We extended our use of ensemble prediction for real-time simulations of the West Africa region using Global Forecasting System (GFS) input for several forecast periods from March 4 to June 7. Instead of varying physics combinations, however, we opted for altering initial conditions, i.e. the specific time at which the simulation was started. As an example (schematic on figure 6), for any given day you have 4 GFS forecasts issued at 00z, 06z, 12z and 18z. Out of those 4 forecasts 2 different forecasts were created. That is, we now have forecasts initialized on a 3-hourly period: 00z, 03z, 06z, etc. This technique yielded important differences in our outlooks that allow for probabilistic forecasts as can be seen in the next section.

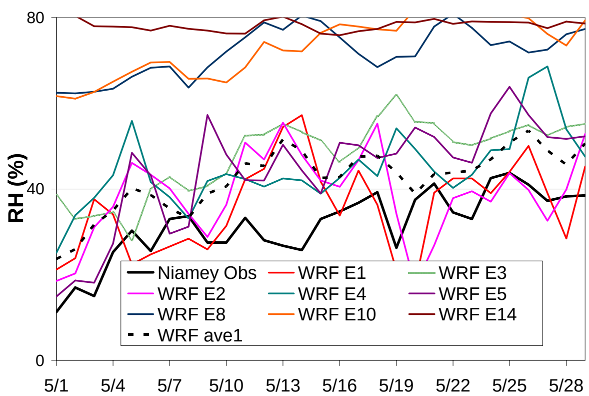

Figure 5. Relative Humidity of as given by an ensemble of WRF simulations using 8 different physics parameter combinations (color), Niamey station observation (black, solid), and LSM ensembles (black, dotted).

Figure 6. Schematic of real-time ensemble technique.

Intraseasonal and Diurnal variability

As we may discern from figure 5, the downscaling of FNL reanalysis captured intraseasonal variability reasonably well, with some ensemble members being able to capture specific events (extreme peaks and valleys in observations) better than others. Similarly, we also present how the model performed in terms of diurnal variability. Figure 7 shows the diurnal pattern of RH (%) for the May 23-29, 2006 period as given by the observations at Niamey [13°27'N, 02°06'E (solid blue)], and two ensemble members E1 (black dashed) and E2 (black dotted). These results also suggest that the model is accurately portraying diurnal variability at this specific location.

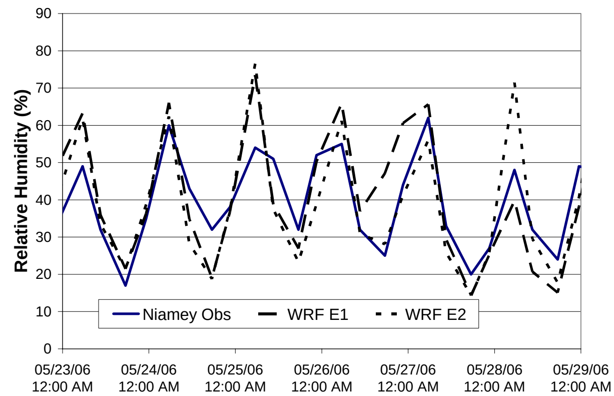

Figure 7. Diurnal variability of RH (%) as given by station data at Niamey (solid blue), and ensemble members E1 (dashed black) and E2 (dotted black).

Real-time Forecasts

We performed a series of real-time ensemble simulation forecasts of relevant variables in an effort to test the capabilities of WRF for usage as a tool in meningitis mitigation efforts in West Africa. We obtained these forecasts using the initial conditions ensembling technique (fig. 6). The physics parameters remained constant and follow those used in ensemble member E2, also described above. We subsequently compared our forecasts against station observations throughout the West Africa region including Niamey as in the above, as well as Kano in Nigeria [12°05'N, 8°53'E (not shown)], Bamako in Mali [12°34'N, 07°55'W (not shown)], among others. Added to station data we also compared our results against gridded NCEP/NCAR reanalysis and our downscaled FNL reanalysis with WRF once the boundary conditions for the forecasted period became available.

In addition to the comparisons discussed above we also developed a website with bi-weekly forecasts generated with our ensemble analysis (climlab.meas.ncsu.edu/westafrica). These include plots showing (i) RH (%) at two meters, (ii) precipitation and 925mb winds, (iii) average surface temperatures and 10m winds and an (iv) a plot of the West Africa region showing daily anomalies of changes in RH (figure 9a). For i-iii above we analyzed both daily and weekly means over the small domain in figure 1. We generated two groups of 8-member forecasts: group 1 for the first 7 days as described in the ensemble prediction section and another for the extended outlook that includes the following week (i.e. 7-15 day forecast). For the extended outlook, GFS provides boundary conditions on a 12-hourly basis, so we varied our initial conditions 36 and 48 hours prior to the start of the forecast period.

We found that real-time simulations are able to capture intraseasonal variability in the moisture regime due to westward-propagating systems. In figure 8 we plotted the observed RH (%) at Niamey, Niger for the March 1 – May 20, 2009 period. In dashed blue vertical lines are days in which the station also reported precipitation. We then focused on two forecast periods adjacent to the rain event on May 7-8 and a spike in RH above the 40% threshold. We note that the forecast initialized on May 1st to allow spin-up time is able to capture the temporary change in the moisture content of the atmosphere at Niamey. The data (not shown) also shows that there was enough spread in the results to provide a probabilistic forecast for this particular event.

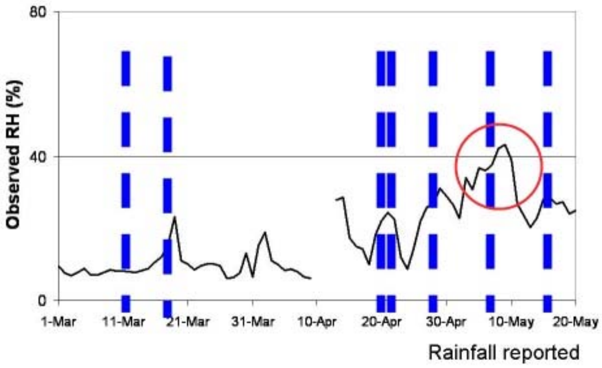

Figure 8. Relative Humidity for the March 1 – May 20 period from a station in Niamey, Niger. Blue dashed vertical lines portray precipitation events.

The implication of transient convective systems on surface moisture is evident in our analysis and WRF allows us to trace the precipitation event on May 7-8 as well as the spike in RH to a westward-propagating disturbance. Figure 9a shows the forecasted change in RH from May 6 to May 7 and a wave-like feature of the 40% threshold (solid black curve) that extends from the 0°E to 10°E with a zenith at 20°N in extreme southern Algeria. The anomalies show positive numbers to the west and corresponding negative numbers on the eastern side of the disturbance. This is another indication that the feature is moving westward. In figure 9b we can discern a significant amount of rainfall extending from northern Ivory Coast sloping eastward into central Niger. It's important to note that these disturbances, although temporary in nature, do increase the moisture in the air (see figure 8) bringing it into a new regime (~20% to ~30%). This is a potentially significant factor for meningitis mitigation efforts in this part of the world and we have showed that WRF simulations are able to capture the event.

Advantage of Dynamical Downscaling

As the 2009 spring season gave way to the summer monsoon, a season-long simulation using FNL boundary conditions was conducted over the region to analyze the limited-area model's performance in diagnosing meningitis risk and also to compare against large scale reanalysis (NCEP/NCAR). The end of the meningitis season also provided us with high resolution information about the disease epidemic, attack rate, and spatiotemporal variance throughout the period (Multi-disease Surveillance Center, 2009). The meningitis data spans the width of the Meningitis Belt but its high resolution information (district scale) is limited to the country of Nigeria. We use data from the district of Kano in north-central Nigeria in terms of the attack rate (No. cases / 100,000 per week) in conjunction with the WRF-derived seasonal information, meteorological observations at Kano and data from the NCEP/NCAR reanalysis to analyze the added value incurred by dynamical downscaling. The data presented here has been averaged for each of the weeks in the meningitis reports.

From figure 10 we note that the attack rate (black-white bars) is higher (~20%) during the beginning of the period (late March through early April) when the observed relative humidity (blue) is below 30%. The attack rate significantly collapses below 8% in mid to late April as the observed relative humidity increases to about 40%, once again suggesting the relationship between moisture and the disease. Fig. 10 also allows us to view two different model-derived analyses of the relative humidity over Kano. The season-long WRF simulation (red) is very close to the observed, thus adding significant value to the use of dynamical downscaling. In contrast, NCEP/NCAR reanalysis (green) overestimates moisture well beyond the observed (by about 20%) during the dry period. When meningitis attack rates are highest, and it also continues to overestimate the relative humidity during the critical moisture onset period in mid to late April.

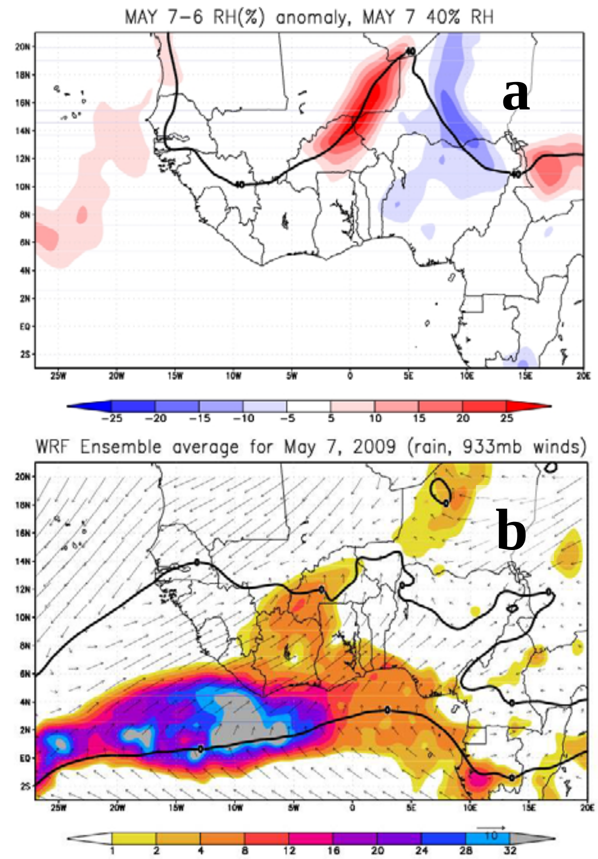

Figure 9. West Africa real-time forecasts for (a) May 7-6 day anomaly for changes in RH (%) and (b) May 7 rain totals (mm) and 933mb winds. The black line shows the position of the ITF and is defined as u wind component equal to zero.

Concluding Remarks

Our analysis above shows that WRF can be used to diagnose the moisture regime preceding the West African Monsoon for health efforts in the region. The back-trajectory analysis has determined that the sources of air mass during the onset of higher moisture into the region are highly variable in horizontal and vertical scales. Further attention needs to be directed towards the variance of large scale patterns that dictate the state of the atmosphere in these source regions. Future work includes ensembling of seasonal predictions for the 2000-2009 period using both physics parameter and initial conditions techniques, data assimilation using WRF3DVAR and a new spectral nudging technique developed at North Carolina State University. High resolution seasonal downscaling of FNL reanalysis will enable us to diagnose long term regional climate drivers, the dynamics of the WAM pre-onset and its relationship with surface moisture (diurnal process, SHL, ITF, large scale circulation patterns, etc), sensitivities (e.g. SST), and other predictive factors like transient systems (which can have a significant influence on the moisture regime at the surface at latitudinal and temporal scales). Time scales generated for useable forecasts relevant to health efforts can be from 2 to 15 days out for the intraseasonal scale and months in advance for the seasonal scale. Further analysis will allow us to look at the different indices appropriate for meningitis mitigation (3,5,7 days of regime change), 40%, 50% + in RH.

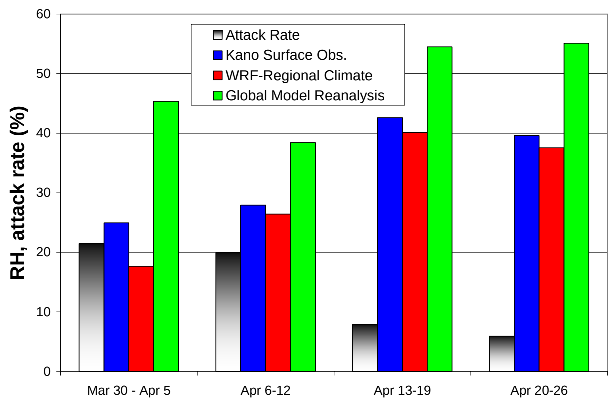

Figure 10. Comparison of meningitis attack rate (black-white), observed relative humidity [blue, (%)], WRF simulation (red) and NCEP/NCAR reanalysis (green).

References

Besancenot, J.P, M. Boko and P.C. Oke, 1997: Weather conditions and cerebrospinal meningitis in Benin (Gulf of Guinea, West Africa) Euro. J of Epidem. **13**: 807–815

Drobinski P, Sultan B, Janicot S. 2005. Role of the Hoggar massif in the West African monsoon onset. *Geophys. Res. Lett.* **32**: L01705

Flamant, C., J.-P. Chaboureau, D. J. Parker, C. M. Taylor, J.-P. Cammas, O. Bock, F. Timouk and J. Pelona, 2007: Airborne observations of the impact of a convective system on the planetary boundary layer thermodynamics and aerosol distribution in the inter-tropical discontinuity region of the West African Monsoon. *Q. J. R. Meteorol. Soc.* **133**: 1175–1189

Flamant, C., P. Knippertz, D. J. Parker,, J.-P. Chaboureau, C. Lavaysse, A. Agusti-Panareda and L. Kergoat, 2009: The impact of a mesoscale convective system cold pool on the northward propagation of the intertropical discontinuity over West Africa. *Q. J. R. Meteorol. Soc.* **135**: 139–159

Greenwood B. (1999) Manson lecture. Meningococcal meningitis in Africa. *Transactions of the Royal Society of Tropical Medicine and Hygiene,* **93**, 341–53.

Hagos, S.M., and K.H. Cook, 2007: Dynamics of the West African monsoon jump. *J. Climate*, **20**, 5264-5284.

Knippertz, P., A.H. Fink, 2009: Prediction of Dry-Season Precipitation in 2 Tropical West Africa and its Relation to Forcing 3 from the Extratropics. *In press*.

Le Barbe´, L., T. Lebel, and D. Tapsoba, 2002: Rainfall variability in West Africa during the years 1950–90. *J. Climate,* **15,** 187–202.

Lebel T, Thorncroft C, Redelsperger J-L. 2005. AMMA white book, available from http://science.amma-international.org/science/.

Molesworth AM, Cuevas LE, Connor SJ, Morse AP and Thomson MC. (2003) Environmental Risk and Meningitis Epidemics in Africa. *Emerging Infectious Diseases* **9(10)**: 1287-1293.

Multi Disease Surveillance Center, 2009: Weekly feedback bulletin on cerebrospinal meningitis, Week 17, 2009. 01 BP 549 Ouagadougou 01, Burkina Faso, http://www.meningvax.org/press-reports.htm

Parker, D.J., R. R. Burton, A. Diongue-Niang, R. J. Ellis, M. Felton, C. M. Taylor, C. D. Thorncroft4, P. Bessemoulin and A. M. Tompkin, 2005: The diurnal cycle of the West African monsoon circulation. *Quart. J. Roy. Meteor. Soc.,* **131**, 2839–2860.

Redelsperger, J.-L., C. D. Thorncroft, A. Diedhiou, T. Lebel, D. J. Parker, and J. Polcher, 2006: African Monsoon Multidisciplinary Analysis: An international research project and field campaign. *Bull. Amer. Meteor. Soc.,* **87,** 1739–1746.

Sultan and S. Janicot, 2000: Abrupt shift of the ITCZ over West Africa and intra-seasonal variability. *Geophys. Res. Lett.,* **27,** 3353–3356.

Sultan and S. Janicot, 2003: The West African Monsoon Dynamics. Part II: The ‘‘Preonset’’ and ‘‘Onset’’ of the Summer Monsoon. *J. Climate.,* **27,** 3353–3356.